TO THE EDITOR:

Clonal hematopoiesis evolves from pretreatment clones and stabilizes after end of chemotherapy in patients with MCL

Christian Winther Eskelund,[1-3,*] Simon Husby,[1-3,*] Francesco Favero,[2,4] Tobias Wirenfeldt Klausen,[5] Francisco German Rodriguez-Gonzalez,[2,4] Arne Kolstad,[6] Lone Bredo Pedersen,[1] Riikka Katariina Räty,[7] Christian H. Geisler,[1] Mats Jerkeman,[8] Joachim Weischenfeldt,[2,4] and Kirsten Grønbæk[1-3]

[1]Department of Hematology, Rigshospitalet, Copenhagen, Denmark; [2]Biotech Research and Innovation Centre and [3]Danish Stem Cell Center, University of Copenhagen, Copenhagen, Denmark; [4]Finsen Laboratory, Rigshospitalet, Copenhagen, Denmark; [5]Hematological Research Laboratory, Herlev University Hospital, Herlev, Denmark; [6]Department of Oncology, Oslo University Hospital, Oslo, Norway; [7]Department of Hematology, Helsinki University Hospital, Helsinki, Finland; and [8]Department of Oncology, Skåne University Hospital, Lund, Sweden

Cytotoxic therapy has been associated with both clonal hematopoiesis (CH) and therapy-related leukemia,[1-3] and mutations in DNA repair genes such as *TP53* and *PPM1D* are strongly associated with prior chemotherapy exposure.[1,4,5] However, data on the origin and longitudinal dynamics of CH during and after chemotherapy are sparse and only exist for smaller, heterogeneous patient cohorts.[6-12] Therefore, in this study, we analyzed the development and evolution of CH in a homogeneous cohort of mantle cell lymphoma (MCL) patients before, during, and after first-line chemotherapy, autologous stem cell transplantation (ASCT), and long-term follow-up after end of therapy.

We investigated 335 DNA samples from 149 patients treated in 2 Nordic Lymphoma Group front-line trials for younger patients (age <66 years) with MCL; MCL2 and MCL3. Both trials consisted of an induction phase of immunochemotherapy followed by consolidation with high-dose chemotherapy (HDT) and ASCT.[13,14] All patients provided written consent, and the study was approved by local ethics committees and conducted in accordance with the Declaration of Helsinki. For initial screening, minimal residual disease (MRD)-negative DNA samples from bone marrow and peripheral blood were collected according to availability (Figure 1A). In patients with detected CH in a screening sample, additional follow-up samples from time points before, during, and after therapy were collected regardless of MRD status (Figure 2A). All samples underwent error-corrected NGS of 21 CH-related genes (supplemental Tables 1 and 2, available on the *Blood* Web site) and general variant calling with a VAF cutoff of 1.0%. Next, consecutive samples from CH^+ patients underwent focused variant calling to identify specific low-frequency mutations already detected in other samples from the same patients (supplemental Methods).

We identified 149 cases with MRD^- bone marrow (n = 134) or peripheral blood (n = 15) samples after HDT-ASCT (Figure 1A). By NGS, we identified 54 CH mutations in 44 (30%) of these samples, with a median VAF of 3.2% (Figure 1B; supplemental Tables 3 and 4). Both prevalence (12%) and clone size (median VAF, 2.4%) were lower in 59 paired MRD^- postinduction samples taken between induction-therapy and HDT-ASCT, indicating a CH-promoting effect of HDT-ASCT (Figure 1C-D). We observed no differences in baseline characteristics between patients with and without CH (supplemental Table 5). Mutations in DNA repair genes (*PPM1D*, n = 4; *TP53*, n = 3; *RAD21*, n = 1; and *BRCC3*, n = 0) were present in only 8 patients (5.4%), fewer than in previous reports.[1,5] We suspect this reflects the lower cumulative dose of chemotherapy received in our cohort of first-line–treated patients compared with the heterogeneous cohort of more heavily pretreated patients published by Gibson et al[1] (median, 2 prior lines of therapy; range, 1-6 prior lines).

With a median follow-up of 8.0 years from ASCT, median overall survival was not influenced by CH (hazard ratio, 0.92; 95% confidence interval, 0.48-1.8; log-rank $P = .82$; Figure 1E). Increasing the VAF cutoff for CH mutations to 2% or 10% did not alter this result (data not shown). Only 4 patients developed TMN disease, with a median time from post-ASCT sample to TMN diagnosis of 30 months (range, 18-42 months), and only 1 of these patients carried a CH mutation in the post-ASCT screening sample (*DNMT3A* P904L; VAF, 1.9%). Of note, compared with the similar study by Gibson et al,[1] in which CH clearly showed poor prognostic impact at time of ASCT, our cohort represented relatively good-risk MCL patients (MRD negativity after ASCT) who all received ASCT in the first line.

Forty-seven patients carried a CH mutation in an MRD^- sample at either the postinduction or post-ASCT time point. In these patients, a total of 77 CH mutations were tracked in the consecutive samples (Figure 2A-B). Comparing 28 paired samples before and after induction chemotherapy, 9 new CH mutations appeared, whereas no mutations disappeared. Of 39 mutations detected at both time points, the median VAF increased from 0.97% (IQR, 0.38%-2.6%) to 1.6% (IQR, 0.90%-3.3%; Wilcoxon $P = .001$), corresponding to a median relative VAF increase of 44% (IQR, −0.88%-230%; Figure 2B). Similarly, comparing 36 postinduction and post-ASCT samples, 3 mutations appeared and 2 disappeared, and the median VAF of 53 shared mutations increased from 1.5% (IQR, 0.91%-3.1%) to 2.8% (IQR, 1.4%-4.8%; $P = .001$), corresponding to a median relative VAF increase of 42% (IQR, −8.0%-157%; Figure 2B).

During induction therapy, the median increment of clones with DNA repair mutations was significantly greater than CH with non-DNA repair mutations (+1.7; IQR, 1.1-3.3 vs +0.48; IQR, 0.008-1.4; Mann-Whitney $P = .008$; Figure 2C; supplemental Figures 1, 3, and 4). In contrast, during HDT-ASCT, expansion of clones with DNA repair mutations was less pronounced and similar to that of clones with non-DNA repair mutations (Figure 2C; supplemental Figures 2-4).

We hypothesized that mutations with relatively more COSMIC references for myeloid malignancies were more likely to represent CH drivers. Mutations with ≥3 COSMIC references compared with <3, respectively, showed a significantly larger increase during HDT-ASCT (+1.4; IQR, 0.61-2.1 vs +0.20; IQR −0.55-1.4;

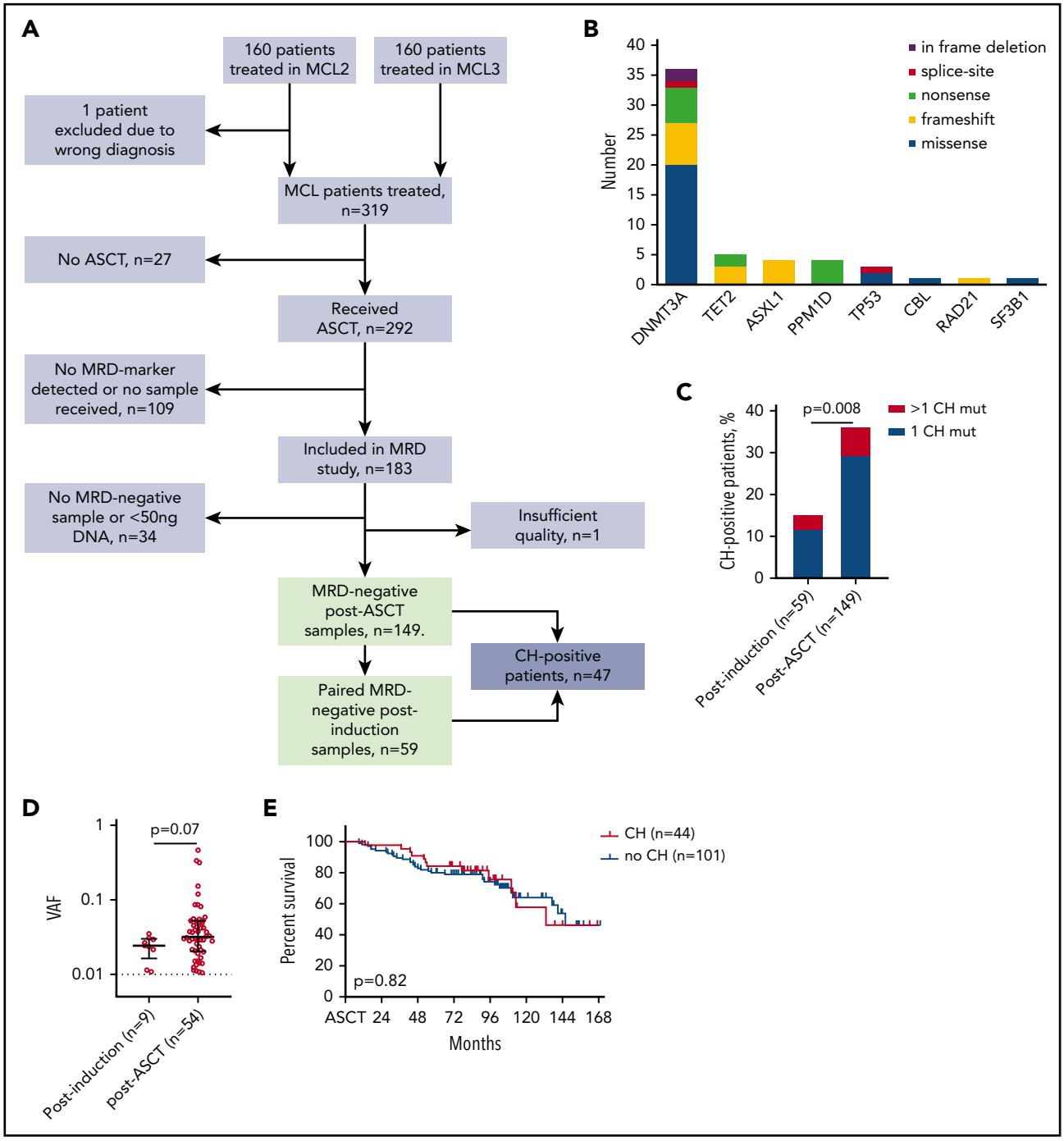

Figure 1. CH mutations detected in the MRD⁻samples of 149 patients. (A) Flowchart of study patients. (B) Landscape of CH mutations in 149 MRD⁻ post-ASCT samples. (C) Prevalence of CH mutations in MRD⁻ samples from postinduction (n = 59) and post-ASCT (n = 149) time points. Statistics by χ^2 test. (D) Variant allele frequency (VAF) of 9 postinduction CH mutations and 54 post-ASCT CH mutations. Analyzed by Mann-Whitney *U* test. (E) Overall survival of patients with and without CH mutations at post-ASCT time point, compared by log-rank test.

P = .029; supplemental Figure 4D). This may represent either an increased resistance to HDT or faster engraftment after ASCT.

During follow-up of 44 CH⁺ patients after end of therapy, 6 new mutations appeared and 6 disappeared. The median interval from post-ASCT to late follow-up sample was 54 months (IQR, 42-57 months). The median VAF of the remaining 62 mutations continued to increase (from 2.9% [IQR, 1.4%-4.7%] to 3.8% [IQR, 1.6%-6.6%]; *P* = .013), but the median growth rate was only 5.1% per year (IQR, −9%-55%), which is likely to reflect an age-related increment (Figure 2D).

Clones carrying DNA repair mutations or mutations with a higher number of COSMIC references did not behave differently after end of therapy (Figure 2C; supplemental Figure 4). However, we observed an overall negative correlation between VAF change

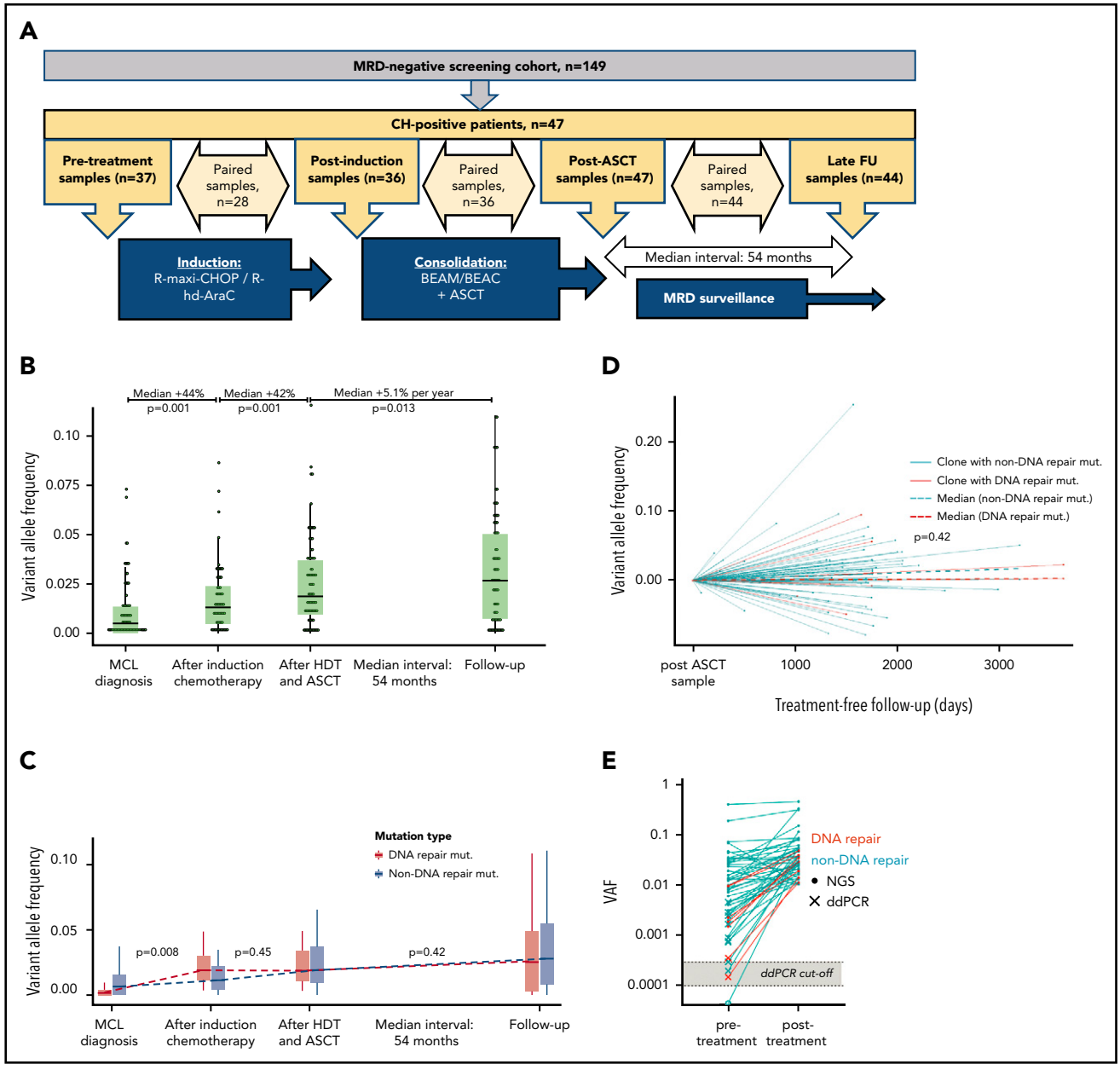

Figure 2. Longitudinal investigation of CH mutations in 47 patients. (A) Overview of samples for longitudinal investigation. (B) Evolution of CH mutation at the 4 time points. Black horizontal lines represent medians; boxes, interquartile ranges (IQRs); and vertical lines, 1.5 × IQRs. Percentages at the top indicate the relative change in VAF size of the CH mutations in paired samples. *P* values were calculated by Wilcoxon rank sum test for paired samples. (C) Evolution of DNA repair mutations (red) and non-DNA repair mutations (turquoise) at the 4 time points. Black horizontal lines indicate medians; boxes, IQRs; and vertical lines, 1.5 × IQRs. *P* values indicate the differences in VAF change between the 2 groups (for paired samples only) by Mann-Whitney *U* test. (D) Evolution of DNA repair (red) and non-DNA repair (turquoise) mutations during chemotherapy-free follow-up. *P* values indicate the comparison of the coefficients of the 2 linear regression models for the DNA repair and non-DNA repair VAFs, respectively. (E) Illustrates the presence of posttreatment CH mutations at the time point before any chemotherapy was administered. Closed circles represent mutations detected by next-generation sequencing (NGS); Xs, mutations detected by droplet digital polymerase chain reaction (ddPCR); and the open circle, the 1 undetected mutation. Gray area represents the range of detection limits for the ddPCR assays; red, DNA repair mutations; turquoise, non-DNA repair mutations. BEAC, carmustine, etoposide, cytarabine, and cyclophosphamide; BEAM, carmustine, etoposide, cytarabine, and melphalan; FU, follow-up; R hd AraC, rituximab plus high-dose cytarabine; R-maxi-CHOP, rituximab, cyclophosphamide (1200 mg/m2), doxorubicin (75 mg/m^2), vincristine (2 mg), prednisolone (100 mg) day 1-5.

during treatment and VAF change during chemotherapy-free follow-up (Spearman's $\rho = -0.32$; 95% CI, −0.53 to −0.064; $P = .013$), suggesting that clones expanding during chemotherapy tend to diminish after end of therapy, possibly because of withdrawal of the selective pressure of chemotherapy (supplemental Figure 5). Fifteen mutations expanded both during treatment and follow-up: 10 DNMT3A mutations (including 3 at the 882 codon), 3 PPM1D mutations, and 2 TET2 mutations. With a median follow-up of 7.7 years (IQR, 6.8-8.8 years), of these 15 patients, none developed TMN disease. We did not find any association between posttreatment behavior of CH clones and VAF size or number of mutations per patient.

To explore the origin of the chemotherapy-associated CH, we investigated the presence of CH clones before exposure to chemotherapy. Selecting all mutations with VAF >1% in postinduction

or post-ASCT samples, 42 (78%) of 54 mutations were detectable by NGS in pretreatment samples. Importantly, exploring the remaining 12 mutations, which were not found by NGS, by sensitive ddPCR, we were able to detect 11 additional mutations. Therefore, taken together, 53 (98%) of 54 posttreatment CH mutations were already detectable before exposure to any chemotherapy (Figure 2E). The undetected mutation (*ASXL1* p.A627fs) occurred a patient who also carried 2 other CH mutations (*ASXL1* p.Arg774fs and *DNMT3A* p.Arg598*). Whether this mutation was in fact induced by chemotherapy or was present at VAF below the detection limit of the ddPCR assay (0.018%) remains unknown (supplemental Table 6). Similarly, we also investigated mutations that seemed to disappear during chemotherapy-free follow-up. By ddPCR, we were able to detect 5 of 6 mutations at a low VAF in the late follow-up samples (supplemental Table 4). Therefore, in total, 66 (99%) of 67 post-ASCT mutations remained detectable during follow-up after end of therapy.

Several previous studies have demonstrated cases where post-chemotherapy CH mutations could be tracked back to a pre-chemotherapy time point.[3,6,8-12,15-17] We here confirm in a large cohort of chemotherapy-naïve patients that nearly all (98%) post-chemotherapy CH mutations could be detected before any treatment was administered, which suggests that CH clones are always expanded, and not induced, by chemotherapy (supplemental Figure 6).

In conclusion, we show for the first time in MRD$^-$ samples from a large, homogeneously treated cohort that CH clones, especially those carrying DNA repair mutations, expand consistently during chemotherapy and HDT-ASCT, whereas CH clones generally stabilize after end of therapy. We found no clinical impact of CH in our cohort of relatively good-risk MCL patients treated in the first-line setting, and thus, our data do not support using CH as a biomarker for choice of treatment in patients undergoing first-line intensive chemotherapy and ASCT. Interestingly, 54 of 55 postchemotherapy CH mutations were already detectable before any chemotherapy was administered. This provides support for a model with expansion of preexisting clones, in a permissive microenvironment, rather than induction of new clones by chemotherapy (supplemental Figure 6).

Acknowledgments

The authors thank the medical and nursing staffs of all contributing departments of the MCL2 and MCL3 trials and the patients for their willingness to participate.

This work was supported by grants from the Independent Research Fund Denmark, Novo Nordisk Foundation, Rigshospitalet's Research Foundation, Lundbeck Foundation, and Danish Cancer Research Foundation. Furthermore, the K.G. laboratory is funded by center grants from the Danish Cancer Society (Danish Research Center for Precision Medicine in Blood Cancer grant 223-A13071-18-S68), the Novo Nordisk Foundation (Novo Nordisk Foundation Center for Stem Cell Biology, DanStem, grant NNF17CC0027852), and the Greater Copenhagen Health Science Partners (Clinical Academic Group in Translational Hematology).

Authorship

Contribution: C.W.E., S.H., K.G., and J.W. conceived and designed the experiments; C.W.E., S.H., F.F., F.G.R.-G., and L.B.P. performed the experiments; C.W.E., S.H., F.F., and T.W.K. analyzed data; M.J., C.H.G., A.K., and R.K.R. conducted the clinical trials, handled patient material, and collected clinical data; C.W.E., S.H., K.G., and J.W. wrote the manuscript; and all authors critically reviewed the final version of the manuscript.

Conflict-of-interest disclosure: The authors declare no competing financial interests.

ORCID profiles: C.W.E., 0000-0002-6409-8081; F.F., 0000-0003-3684-2659; F.G.R.-G., 0000-0002-8509-0804; J.W., 0000-0002-3917-5524; K.G., 0000-0002-1535-9601.

Correspondence: Kirsten Grønbæk, Department of Hematology, Rigshospitalet, Copenhagen, Denmark; e-mail: kirsten.groenbaek@regionh.dk.

Footnotes

*C.W.E. and S.H. contributed equally to this work.

For original data, please e-mail the corresponding author.

The online version of this article contains a data supplement.

There is a *Blood* Commentary on this article in this issue.

REFERENCES

1. Gibson CJ, Lindsley RC, Tchekmedyian V, et al. Clonal hematopoiesis associated with adverse outcomes after autologous stem-cell transplantation for lymphoma. *J Clin Oncol*. 2017;35(14):1598-1605.

2. Gillis NK, Ball M, Zhang Q, et al. Clonal haemopoiesis and therapy-related myeloid malignancies in elderly patients: a proof-of-concept, case-control study. *Lancet Oncol*. 2017;18(1):112-121.

3. Takahashi K, Wang F, Kantarjian H, et al. Preleukaemic clonal haemopoiesis and risk of therapy-related myeloid neoplasms: a case-control study. *Lancet Oncol*. 2017;18(1):100-111.

4. Kahn JD, Miller PG, Silver AJ, et al. *PPM1D*-truncating mutations confer resistance to chemotherapy and sensitivity to PPM1D inhibition in hematopoietic cells. *Blood*. 2018;132(11):1095-1105.

5. Coombs CC, Zehir A, Devlin SM, et al. Therapy-related clonal hematopoiesis in patients with non-hematologic cancers is common and associated with adverse clinical outcomes. *Cell Stem Cell*. 2017;21(3):374-382.e4.

6. Wong TN, Miller CA, Jotte MRM, et al. Cellular stressors contribute to the expansion of hematopoietic clones of varying leukemic potential. *Nat Commun*. 2018;9(1):455.

7. Arends CM, Galan-Sousa J, Hoyer K, et al. Hematopoietic lineage distribution and evolutionary dynamics of clonal hematopoiesis. *Leukemia*. 2018;32(9):1908-1919.

8. Berger G, Kroeze LI, Koorenhof-Scheele TN, et al. Early detection and evolution of preleukemic clones in therapy-related myeloid neoplasms following autologous SCT. *Blood*. 2018;131(16):1846-1857.

9. Ortmann CA, Dorsheimer L, Abou-El-Ardat K, et al. Functional dominance of CHIP-mutated hematopoietic stem cells in patients undergoing autologous transplantation. *Cell Rep*. 2019;27(7):2022-2028.e3.

10. Wong TN, Ramsingh G, Young AL, et al. Role of TP53 mutations in the origin and evolution of therapy-related acute myeloid leukaemia. *Nature*. 2015;518(7540):552-555.

11. Wong TN, Miller CA, Klco JM, et al. Rapid expansion of preexisting nonleukemic hematopoietic clones frequently follows induction therapy for de novo AML. *Blood*. 2016;127(7):893-897.

12. Young AL, Wong TN, Hughes AEO, et al. Quantifying ultra-rare pre-leukemic clones via targeted error-corrected sequencing. *Leukemia*. 2015;29(7):1608-1611.

13. Geisler CH, Kolstad A, Laurell A, et al; Nordic Lymphoma Group. Long-term progression-free survival of mantle cell lymphoma after intensive front-line immunochemotherapy with in vivo-purged stem cell rescue: a nonrandomized phase 2 multicenter study by the Nordic Lymphoma Group. *Blood*. 2008;112(7):2687-2693.

14. Kolstad A, Laurell A, Jerkeman M, et al; Nordic Lymphoma Group. Nordic MCL3 study: 90Y-ibritumomab-tiuxetan added to BEAM/C in non-CR patients before transplant in mantle cell lymphoma. *Blood*. 2014;123(19):2953-2959.

15. Desai P, Mencia-Trinchant N, Savenkov O, et al. Somatic mutations precede acute myeloid leukemia years before diagnosis. *Nat Med*. 2018;24(7):1015-1023.

16. Abelson S, Collord G, Ng SWK, et al. Prediction of acute myeloid leukaemia risk in healthy individuals. *Nature*. 2018;559(7714):400-404.

17. Young AL, Tong RS, Birmann BM, Druley TE. Clonal haematopoiesis and risk of acute myeloid leukemia. *Haematologica*. 2019;104(12):2410-2417.

DOI 10.1182/blood.2019003539

TO THE EDITOR:

EBV$^+$ diffuse large B-cell lymphoma associated with chronic inflammation expands the spectrum of breast implant–related lymphomas

Lénaïg Mescam,[1] Vincent Camus,[2,3] Jean-Marc Schiano,[4] José Adélaïde,[5] Jean-Michel Picquenot,[6] Arnaud Guille,[5] Marie Bannier,[7] Philippe Ruminy,[3] Pierre-Julien Viailly,[3] Fabrice Jardin,[2,3] Reda Bouabdallah,[4] Isabelle Brenot-Rossi,[8] Elodie Bohers,[3] Cyrielle Robe,[9] Camille Laurent,[10] Daniel Birnbaum,[5] Andrew Wotherspoon,[11] Philippe Gaulard,[9,*] and Luc Xerri[12,*]

[1]Department of Biopathology, Institut Paoli Calmettes, Marseille, France; [2]Department of Hematology, Centre Henri Becquerel, Rouen, France; [3]INSERM U1249, Centre Henri Becquerel, Rouen, France; [4]Department of Hematology, Institut Paoli Calmettes, Marseille, France; [5]Department of Molecular Oncology, Institut Paoli-Calmettes, Centre de Recherche en Cancérologie de Marseille, INSERM U1068, Centre National de la Recherche Scientifique Unité Mixte de Recherche (UMR) 7258, Aix-Marseille University, UM 105, Marseille, France; [6]Department of Pathology, Centre Henri Becquerel, Rouen, France; [7]Department of Surgical Oncology, Institut Paoli Calmettes, Marseille, France; [8]Department of Nuclear Imaging, Institut Paoli Calmettes, Marseille, France; [9]Department of Pathology, INSERM U955, Hôpital Henri Mondor, Créteil, France; [10]Department of Pathology, CHU Toulouse, IUCT Oncopole, INSERM, UMR 1037 Centre de Recherche en Cancerologie de Toulouse, Laboratoire D'Excellence Toulouse Cancer (TOUCAN), Paul Sabatier University Toulouse III, Toulouse, France; [11]Department of Pathology, Royal Marsden Hospital, London, United Kingdom; and [12]Department of Biopathology and Tumor Immunology, Institut Paoli-Calmettes, Centre de Recherche en Cancérologie de Marseille, INSERM U1068, Centre National de la Recherche Scientifique UMR 7258, Aix-Marseille University, UM105, Marseille, France

Breast implant–associated anaplastic large cell lymphoma (BI-ALCL) has emerged as a new provisional entity in the revised 2016 World Health Organization classification of lymphoid malignancies.[1] BI-ALCL is a rare T-cell lymphoma arising adjacent to breast implants and composed of large atypical CD30$^+$ cells frequently confined to the peri-implant seroma fluid and adjacent capsule, more rarely forming a solid infiltrating mass.[2,3] So far, only exceptional cases of lymphomas other than BI-ALCL have been reported to occur in the vicinity of breast implants, including miscellaneous B-cell lymphomas.[4-7] It remains so far unclear whether these cases are coincidental or could be related to breast implants.

We report 3 cases of Epstein-Barr virus (EBV)$^+$ diffuse large B-cell lymphomas (DLBCLs) occurring in contact with breast implants. These cases were also characterized by various degrees of invasion of the periprosthetic capsule but no tumor mass, which make them distinct from classical primary breast DLBCLs.[8,9] To our knowledge, no series of DLBCL adjacent to breast implants has been documented so far. This study was approved by the institutional review board of the Institut Paoli-Calmettes, and all patients gave their informed consent.

In the 3 patients (aged 61 to 72 years), the diagnosis was allowed by excision of the periprosthetic capsule due to esthetical issues in cases 1 and 3 or incidental positron emission tomography (PET) scanner during breast cancer surveillance in case 2 (Table 1). In all cases, the lymphoma tumor was strictly confined to the capsule surrounding breast implants (macrotextured type from Allergan), and the PET computed tomography finding was negative otherwise. The bone marrow biopsy result was also negative. No seroma had been observed prior to capsulectomy in any case, which prevented any fluid aspiration and cytologic analysis. None of the patients had any known immunodeficiency or pharmacologic immunosuppression.

Formalin-fixed and paraffin-embedded capsulectomy samples from the 3 cases were extensively characterized using histological, phenotypical, cytogenetic, and molecular analyses, including targeted next-generation sequencing (tNGS) and array comparative genomic hybridization (aCGH), as described in supplemental Materials and methods (available on the *Blood* Web site). Clinicopathological and biological features of the 3 cases are detailed in Table 1 and supplemental Tables 1 to 4 and illustrated in Figure 1 and supplemental Figure 1.

The 3 cases shared common pathological features consisting of sheets, clusters, and ribbons of large pleomorphic CD30$^+$ EBV-infected B-cells, with EBER expression in virtually all lymphoma cells. The latency profile was type III (LMP1$^+$/EBNA-2$^+$) in 2 cases, whereas the remaining case was negative for both LMP1 and EBNA2. Postresection plasma EBV levels were positive in the 2 analyzed cases, with a decrease over time (supplemental Table 1). Lymphoma cells were observed on the luminal side of the capsule or suspended in a fibrinoid material with constant thickening and invasion of the capsule. This invasion formed cell